

Absorber and gain chip optimization to improve performance from a passively modelocked electrically pumped vertical external cavity surface emitting laser

C. A. Zaugg,^{1,a)} S. Gronenborn,² H. Moench,² M. Mangold,¹ M. Miller,³ U. Weichmann,² W. P. Pallmann,¹ M. Golling,¹ B. W. Tilma,¹ and U. Keller¹

¹Department of Physics, Institute for Quantum Electronics, ETH Zürich, 8093 Zürich, Switzerland

²Philips Technologie GmbH Photonics Aachen, Steinbachstrasse 15, 52074 Aachen, Germany

³Philips Technologie GmbH U-L-M Photonics, Lise-Meitner-Strasse 13, 89081 Ulm, Germany

(Received 21 February 2014; accepted 18 March 2014; published online 28 March 2014)

We present an electrically pumped vertical-external-cavity surface-emitting laser (EP-VECSEL) modelocked with a semiconductor saturable absorber mirror (SESAM) with significantly improved performance. In different cavity configurations, we present the shortest pulses (2.5 ps), highest average output power (53.2 mW), highest repetition rate (18.2 GHz), and highest peak power (4.7 W) to date. The simple and low-cost concept of EP-VECSELs is very attractive for mass-market applications such as optical communication and clocking. The improvements result from an optimized gain chip from Philips Technologie GmbH and a SESAM, specifically designed for EP-VECSELs. For the gain chip, we found a better trade-off between electrical and optical losses with an optimized doping scheme in the substrate to increase the average output power. Furthermore, the device's bottom contact diameter (60 μm) is smaller than the oxide aperture diameter (100 μm), which favors electro-optical conversion into a TEM₀₀ mode. Compared to optically pumped VECSELs we have to increase the field enhancement in the active region of an EP-VECSEL which requires a SESAM with lower saturation fluence and higher modulation depth for modelocking. We therefore used a resonant quantum well SESAM with a 3.5-pair dielectric top-coating (SiN_x and SiO₂) to enhance the field in the absorber at the lasing wavelength of 980 nm. The absorption bandedge at room temperature is detuned (965 nm) compared to the resonance (980 nm), which enables temperature-tuning of the modulation depth and saturation fluence from approximately 2.5% up to 15% and from 20 $\mu\text{J}/\text{cm}^2$ to 1.1 $\mu\text{J}/\text{cm}^2$, respectively. © 2014 Author(s). All article content, except where otherwise noted, is licensed under a Creative Commons Attribution 3.0 Unported License. [<http://dx.doi.org/10.1063/1.4870048>]

Optically pumped (OP) vertical-external-cavity surface-emitting lasers (OP-VECSELs),¹ also referred to as OP semiconductor disk lasers (OP-SDL), have evolved to powerful laser sources offering a continuous wave (cw) average output power beyond the 100 W level (multimode).² Passively modelocked with a semiconductor saturable absorber mirror (SESAM)³ makes VECSELs a compact,^{4,5} low-noise^{6,7} emitter of ultrashort pulses in a repetition rate range from <100 MHz⁸ to 50 GHz⁵ (fundamental modelocking) or even 175 GHz in harmonic modelocking.⁹ Sub-100 fs pulses in burst operation,¹⁰ 107 fs in fundamental modelocked operation with a few mW of average power,¹¹ and multi-Watt level average output power with a few hundred fs-pulses^{12–14} have been demonstrated recently for wavelengths around 1 μm . As semiconductor gain allows for band-gap engineering, modelocking was demonstrated in various other wavelength ranges, e.g., in red,^{15,16} at 1.2 μm ¹⁷ or at 2 μm .¹⁸

Since both the VECSEL gain chip and the saturable absorber are based on semiconductor materials, they can be combined into one chip, which is referred to as the MIXSEL (modelocked integrated-external-cavity surface-emitting laser).¹⁹ Record high performance has been reported from optically pumped MIXSELs, e.g., the highest average power

of 6.4 W with picosecond pulses,²⁰ femtosecond pulses,²¹ fundamental modelocking from 5 to >100 GHz repetition rates,²² or record low timing jitter performance.²³ With the MIXSEL, modelocked SDLs made a significant improvement in compactness and complexity.²³

A practical alternative approach for more compact VECSELs is to use electrical pumping (EP-VECSELs),^{24–26} which can intrinsically be implemented in semiconductor lasers. This reduces the complexity, the footprint, and the costs of these lasers drastically. Compared to vertical surface-emitting lasers (VCSELs),^{27,28} EP-VECSELs offer the possibility for power scaling^{25,29} while maintaining higher beam quality and brightness. However, compared to OP-VECSELs, the performance of EP-VECSELs is limited by the fundamental trade-off between electrical and optical losses: higher doping reduces the electrical resistance and therefore leads to a lower thermal load, thus increasing the maximum output power; on the other hand, the higher doping induces a higher free-carrier absorption (FCA) thus limiting the output power.²⁵ Nevertheless, up to 500 mW in TEM₀₀ cw operation was demonstrated from EP-VECSELs (i.e., the NECSEL from Novalux) in 2003.²⁴ With the same chips, first passive modelocking results were presented with up to 40 mW in 57-ps pulses,³⁰ 15-ps pulses with some tens of mW and a repetition rate of up to 15 GHz.³¹ In 2012, we

^{a)}Electronic mail: zauggc@phys.ethz.ch



presented sub-10-ps pulses in collaboration with Philips Technologie GmbH.³² Shortly after, pulses as short as 6.3 ps with an average output power of 6.2 mW or a peak power of more than 1 W were demonstrated with chips designed, grown, and fabricated at ETH.²⁹

The previous results indicated that a better trade-off between the electrical and optical properties of the gain chip combined with an improved SESAM could potentially generate both shorter pulse durations and higher average output powers.^{29–32} Based on our prior experience, we used an improved SESAM, specifically designed for EP-VECSELS, to obtain modelocking with the new gain chip³³ from Philips Technologie GmbH, optimized for fundamental-transverse mode at high output power (up to 90 mW). As a result, we set benchmarks to the peak and average output power, pulse duration and repetition rate from modelocked EP-VECSELS: pulses as short as 2.5 ps, average output power up to 53.2 mW, and repetition rates of up to 18.2 GHz were obtained with a SESAM modelocked EP-VECSEL in different cavity configurations. As the electrical pumping scheme allows for extremely compact packaging with footprints down to a few mm² for the 18-GHz cavity, passively modelocked EP-VECSELS could be considered as interesting candidates for mass-market applications such as optical communication,³⁴ sampling,³⁵ and clocking.³⁶

We use the latest generation EP-VECSEL gain chip fabricated by Philips Technologie GmbH based on the concept and design presented in 2014³³ and similar to the ones previously used for modelocking.³² The basic structure chosen for this gain chip is referred to as a bottom emitter, meaning that the light is emitted through the substrate of the semiconductor layer stack. This processing scheme allows for bonding the bottom mirror directly onto the heat sink and thus enables an efficient thermal management, which is crucial for high-power operation. After processing, the EP-VECSEL gain chip consists of the following elements (listed from bottom to top): An AlN heat spreader; a bottom contact with a diameter (BCD) of 60 μm ; an AlGaAs 37-pair p-doped distributed Bragg reflector (p-DBR) serving as bottom mirror; the active region consisting of 3 InGaAs quantum wells (QWs) embedded in GaAs; an intermediate n-doped DBR with 11 pairs; an oxide aperture with a diameter of 100 μm ; the substrate thinned down to 100 μm ; a top ring electrode and a single-layer dielectric anti-reflection (AR) coating. The two major improvements (compared to the Philips chips previously presented)³² can be summarized as follows. First, an optimized doping scheme is implemented leading to a better trade-off between electrical and optical losses. In particular, the n-doping of the substrate is reduced from $11 \times 10^{16} \text{ cm}^{-3}$ to $5.7 \times 10^{16} \text{ cm}^{-3}$ resulting in an increase of both the average power and efficiency of more than 10%.³³ Second, the BCD (60 μm) was chosen to be smaller than the oxide aperture (100 μm), which strongly confines the current injection profile in the center, whereas the vertical waveguide due to the refractive index change of the oxidized layer is still wide enough not to distort the resonator mode. Therefore, a higher fundamental-transversal mode (TEM₀₀) power is supported,³³ which was previously identified as a major limiting factor for modelocking performance.^{25,29}

For passive modelocking of the EP-VECSEL, the non-linear properties of the SESAM need to be adapted properly to the highly resonant gain chip. The critical parameters are the modulation depth ΔR and the saturation fluence F_{sat} . For a given QW absorber at a fixed temperature and wavelength, the product $\Delta R \times F_{\text{sat}}$ is constant for different field enhancements at the absorber position ζ_{abs} , i.e., the field intensity relative to the incoming field intensity of 1.^{21,37,38} For instance, a high ζ_{abs} (meaning an enhanced resonance in the SESAM) leads to a low F_{sat} at a high ΔR and vice versa. This allows for designing ζ_{abs} in order to satisfy an optimum trade-off within the limitations of the semiconductor's intrinsic dynamic gain saturation.^{32,39,40} Its influence on VECSELS with a high gain enhancement ζ_{gain} is critical for the modelocking performance: A SESAM with a low F_{sat} enables to saturate the absorber faster than the gain which opens a larger net gain window and thus leads to higher power. This is particularly important for the EP-VECSEL gain chips where the strong ζ_{gain} results in an $F_{\text{sat,gain}}$ of about $6 \mu\text{J}/\text{cm}^2$.³² Previously, a SESAM with a too high F_{sat} was identified as one of the factors that limited the laser performance. As mentioned above, a lower F_{sat} is linked to a higher ΔR which will eventually inhibit laser operation if it is equal to or higher than the small signal gain.^{4,39} However, for EP-VECSELS a high ΔR is tolerated due to the high gain (>10%)³² and even beneficial because it prevents the laser from multi-pulse modelocked operation and instabilities. Therefore, a ΔR significantly higher than 1% (as previously used)^{29,32} and a lower F_{sat} is expected to improve both the modelocking stability and performance.

Following these considerations, we fabricated a SESAM with a low F_{sat} and a high ΔR as follows. The semiconductor layer stack consisted of a 30-pair AlAs/GaAs DBR followed by a single InGaAs QW absorber embedded in AlAs and placed in an antinode of the standing wave pattern of the electric field. A thin GaAs layer ends the structure completely anti-resonant (electric field node at the semiconductor-air interface). At 25 °C, the absorption of the QW finds its maximum at 965 nm, shifting with approximately 0.32 nm/K.²¹ The DBR is designed for 960 nm with a ζ_{abs} of the uncoated SESAM of 0.34 (normalized to the incoming field intensity of 1). To reduce the F_{sat} and enhance the ΔR , we coated the semiconductor with SiN_x and SiO₂ using a plasma enhanced chemical vapor deposition (PECVD) reactor. To achieve a maximum resonance at $\lambda \approx 980 \text{ nm}$ (the laser's operation wavelength), we chose 7 layers with thicknesses as follows (starting from the semiconductor side): 135.2 nm SiN_x followed by 3 pairs of $\lambda/4$ -layers of SiO₂ (168.9 nm) and SiN_x (128.7 nm). This layer sequence leads to a theoretical ζ_{abs} of 6.5, i.e., an enhancement of 20 compared to the as-grown structure. Since the layers grown by PECVD suffer from thickness variations of up to 5% per individual layer, the resulting ζ_{abs} is difficult to estimate. However, the crucial parameters ΔR and F_{sat} are experimentally accessible with our high precision non-linear reflectivity measurement setup.⁴¹ We use a commercial modelocked Ti:Sapphire laser emitting 110 fs-pulses at a center wavelength of 980 nm to characterize the SESAM. At 25 °C, the top-coated SESAM exhibits a $\Delta R = 2.9\%$ and an $F_{\text{sat}} = 3.1 \mu\text{J}/\text{cm}^2$. With increasing temperature, the QW's absorption overlaps more and more with the

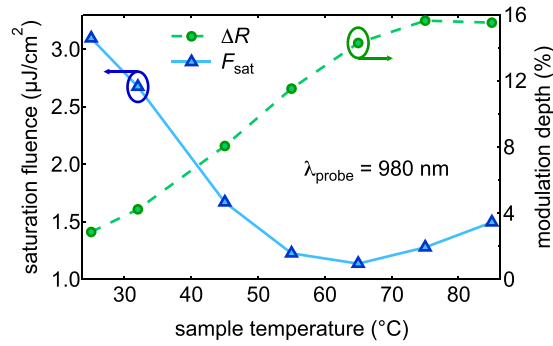


FIG. 1. Temperature dependent SESAM parameters: saturation fluences F_{sat} (blue triangles, left axis) and modulation depths ΔR (green circles, right axis) measured at 980 nm with 110 fs pulses.

structure's resonance resulting in a maximum $\Delta R = 15.7\%$ (at 75°C , $F_{\text{sat}} = 1.3 \mu\text{J}/\text{cm}^2$) and a minimum $F_{\text{sat}} = 1.1 \mu\text{J}/\text{cm}^2$ (at 65°C , $\Delta R = 14.3\%$). The temperature dependent measurement is shown in Fig. 1.

Due to the low field of the uncoated SESAM ($\zeta_{\text{abs,noTC}} = 0.34$), ΔR_{noTC} is close to the measurement precision (0.1%) at 25°C . At 75°C (where the highest signal is present) we measured $\Delta R_{\text{noTC}} \approx 1.2\%$, i.e., about a factor of 13 lower compared to the top-coated sample. Because ΔR scales with the electric field, we can calculate the field enhancement of the top-coated SESAM to $\zeta_{\text{abs}} \approx 4.4$. In addition to the nonlinear reflectivity, we characterized the recovery dynamics with a time-resolved differential reflectivity technique using the same Ti:Sapphire laser. The experiment revealed a fast (intra-band thermalization) and slow (inter-band relaxation) absorption time constant $\tau_{\text{fast}} \approx 250$ fs and $\tau_{\text{slow}} \approx 2$ ps, respectively (at 980 nm and room temperature).

We used the following three cavity geometries to modelock the EP-VECSEL. A long and a short version of a V-shaped cavity with a SESAM and a curved output coupler (OC) as the end mirrors and the gain chip as folding mirror. Furthermore, we used a Z-shaped cavity with a curved high reflector (HR) as an additional folding mirror. In the two V-cavities, the SESAM was placed at a distance of ≈ 3 mm from the gain chip. The OC with a radius of curvature (ROC) of 15 mm (10 mm for the short cavity) was at a distance of ≈ 13.3 mm (≈ 5 mm) from the gain chip leading to a total cavity length of ≈ 16.3 mm (≈ 8 mm) and a pulse repetition rate of 9.2 GHz (18.75 GHz). The mode size radii were

designed to be approximately $50 \mu\text{m}$ on the gain chip and slightly smaller, i.e., 30 to $45 \mu\text{m}$ on the SESAM in order to enhance the saturation and thus exploit the optimum modulation. The exact beam waists are difficult to estimate due to a strong, pump-current dependent thermal lens. But since we aligned the cavity simultaneously for modelocking performance and beam quality, the thermal lens is optimally compensated for each configuration. For the Z-cavity, we used a folding mirror with a ROC of 15 mm at a distance of ≈ 14 mm from the SESAM and ≈ 19 mm from the gain chip, respectively. The OC with a ROC of 38 mm was placed ≈ 35 mm from the gain chip, leading to a total cavity length of ≈ 68 mm and a pulse repetition rate of 2.2 GHz. We estimate the mode size radii in this case to be $50 \mu\text{m}$ on the gain chip and $35 \mu\text{m}$ on the SESAM. An AR-coated, $20 \mu\text{m}$ thick fused silica etalon was used for polarization control, except in the 18-GHz cavity.

We achieved stable fundamental modelocking using a variety of laser configurations. Figure 2 shows a measurement set of the highest average output power of 53.2 mW emitted from the 9.2-GHz cavity using an OC of 11% (ROC 15 mm) at a pump current of 355 mA. The microwave spectrum detected with a fast photodiode is shown in Fig. 2(a). With an autocorrelator we measured a pulse duration of 2.9 ps, see Fig. 2(b), and verified fundamental modelocking (inset). The pulses are nearly transform limited and centered around 981 nm as measured with an optical signal analyzer shown in Fig. 2(c). The heat sink temperature of the gain chip and the SESAM was kept at 3°C and 32°C (see Fig. 1), respectively.

Using the OC with a ROC of 10 mm (OC transmission of 5%) in a shorter cavity enabled modelocking at 18.2 GHz with 10.1 mW of average output power at an injection current of 265 mA. Clean microwave spectra in a wide and narrow span are shown in Figs. 3(a) and 3(b), respectively. The pulse duration was measured to be 9.7 ps as shown in the autocorrelation of the pulse train in Fig. 3(c). No background is present between two pulses, thus confirming fundamental modelocking with clearly separated pulses. For this laser, the gain chip and SESAM heat sink temperatures were stabilized at 3°C and at 25°C (see Fig. 1), respectively. We emphasize that the volume containing the essential elements for this cavity (i.e., OC mirror with mount, gain chip on heatsink, and SESAM on mount) is only $\sim 3 \times 3 \times 2 \text{ cm}^3$. If

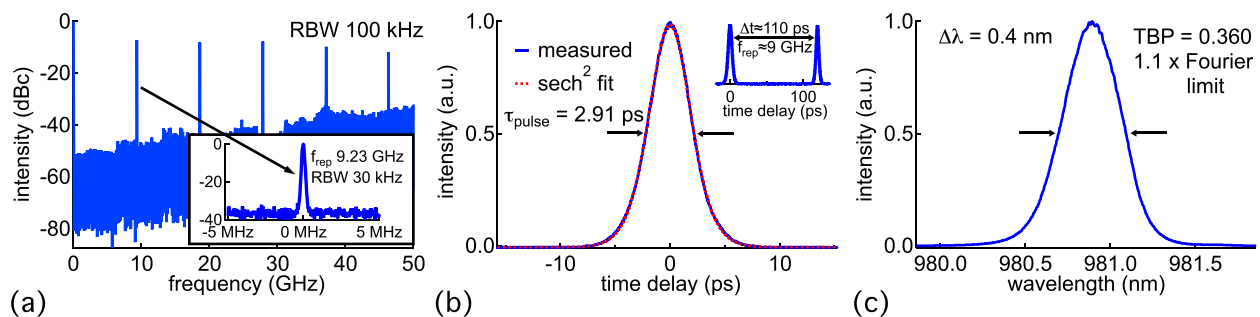


FIG. 2. SESAM modelocked EP-VECSEL with highest average output power of 53.2 mW. (a) Microwave spectrum of the pulse train in a wide span and zoomed in around the fundamental pulse repetition frequency of 9.23 GHz (inset). (b) Autocorrelation (blue) and sech^2 -fit (red dashed) revealing a pulse duration of 2.9 ps. We verified fundamental modelocking with a longer time delay (inset). (c) Optical spectrum showing a clean and a close to transform-limited spectral width. (TBP: time-bandwidth product.)

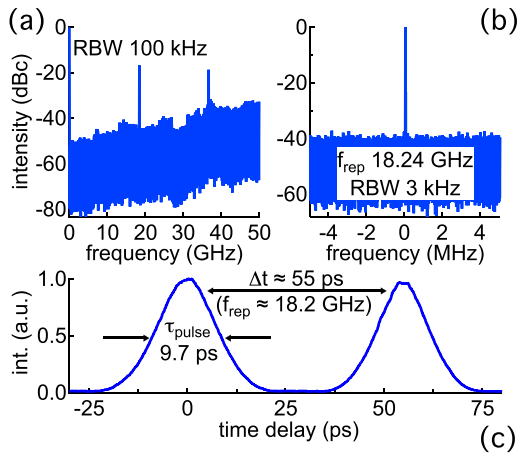


FIG. 3. SESAM modelocked EP-VECSEL pulse train at repetition rate of 18.2 GHz with an average output power of 10.1 mW. (a) Microwave spectrum in a wide span and (b) zoomed in around the fundamental pulse repetition frequency. (c) Autocorrelation of the pulse train indicating 9.7 ps-pulses separated by ≈ 55 ps, confirming fundamental modelocking at >18 GHz.

optimized for compactness, the laser could be built in a volume as small as 1 cm^3 with little effort, and even smaller if industrial packaging would be applied.

The shortest pulses were achieved with the Z-cavity described above using an OC transmission of 7%. The laser was operated at a pump current of 282 mA at a gain chip and SESAM temperature of 10.6°C and 55°C (see Fig. 1), respectively. As shown in Fig. 4(a), we measured pulses as short as 2.47 ps with an average output power of 15.9 mW. The optical spectrum is centered around 981 nm (Fig. 4(b)) and the repetition rate is 2.17 GHz.

Using slightly different current (288.7 mA) and temperature settings (gain chip: 9.7°C ; SESAM: 55°C) and aligning the same cavity for maximum peak power resulted in 3-ps pulses at a repetition rate of 2.15 GHz with an output power of 35 mW. The corresponding peak power is 4.7 W. Table I summarizes the modelocking results.

In conclusion, we presented improved modelocking results of EP-VECSELs in different cavity configurations, i.e., the shortest pulses (2.5 ps), highest average (53.2 mW),

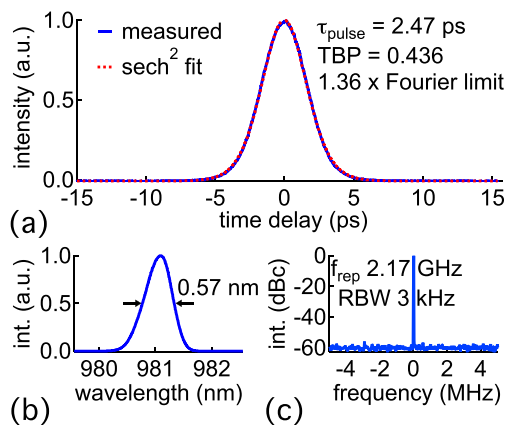


FIG. 4. SESAM modelocked EP-VECSEL with the shortest pulses with an average output power of 16 mW. (a) Autocorrelation trace and sech^2 -fit revealing 2.47 ps pulses with a slight chirp. (b) Optical spectrum centered around 981 nm. (c) Microwave spectrum of the pulse train showing a repetition rate of 2.17 GHz. (TBP: time-bandwidth product.)

TABLE I. Overview of the results presented in this paper.

P_{avg} (mW)	f_{rep} (GHz)	τ_{pulse} (ps)	P_{peak} (W)
53.2	9.2	2.91	1.74
10.1	18.2	9.48	0.05
15.9	2.2	2.47	2.62
35.0	2.2	3.03	4.73

peak power (4.7 W), and the highest repetition rate (18.2 GHz). The gain chip, optimized for high TEM_{00} -power, enabled the increase of average output power. In addition, we used an optimized SESAM with the correctly adapted nonlinear properties, i.e., a low F_{sat} and a high ΔR , both finely adjusted by temperature. But as much as this SESAM is essential to explain the short pulses, it is not sufficient. As reported recently for OP-VECSELs, the total group delay dispersion (GDD) per cavity round-trip needs to be managed carefully.⁴⁰ However, for resonant gain chips and SESAMs, the GDD can neither be calculated nor measured very precisely. Therefore, we can only assume that by aligning and tuning the EP-VECSEL for the shortest pulses (e.g., cavity alignment, injection current, and chip temperatures), a laser cavity configuration with a small absolute GDD value was found, thus explaining the low chirp (Fig. 4(a)). In this case, the pulse duration was only restricted by the gain bandwidth, which is limited by the high finesse of the Fabry-Pérot cavity formed by the resonant sub-cavity around the active region. By reducing the reflectivity of the intermediate n-DBR, the gain bandwidth can be broadened, but only at the expense of a lower small-signal gain. Therefore, a trade-off between average output power and pulse duration is always present in an EP-VECSEL.

The authors acknowledge support of the technology and cleanroom facility FIRST of ETH Zurich for advanced micro- and nanotechnology. This work was financed by the Swiss Confederation Program Nano-Tera.ch, which was scientifically evaluated by the Swiss National Science Foundation (SNSF).

¹M. Kuznetsov, F. Hakimi, R. Sprague, and A. Mooradian, *IEEE Photonics Technol. Lett.* **9**(8), 1063–1065 (1997).

²B. Heinen, T. L. Wang, M. Sparenberg, A. Weber, B. Kunert, J. Hader, S. W. Koch, J. V. Moloney, M. Koch, and W. Stolz, *Electron. Lett.* **48**(9), 516–517 (2012).

³U. Keller, *Nature* **424**, 831–838 (2003).

⁴U. Keller and A. C. Tropper, *Phys. Rep.* **429**(2), 67–120 (2006).

⁵D. Lorenser, D. J. H. C. Maas, H. J. Unold, A.-R. Bellancourt, B. Rudin, E. Gini, D. Ebling, and U. Keller, *IEEE J. Quantum Electron.* **42**(8), 838–847 (2006).

⁶A. H. Quarterman, K. G. Wilcox, S. P. Elsmere, Z. Mihoubi, and A. C. Tropper, *Electron. Lett.* **44**(19), 1135–1137 (2008).

⁷V. J. Wittwer, C. A. Zaugg, W. P. Pallmann, A. E. H. Oehler, B. Rudin, M. Hoffmann, M. Golling, Y. Barbarin, T. Sudmeyer, and U. Keller, *IEEE Photonics J.* **3**(4), 658–664 (2011).

⁸C. A. Zaugg, A. Klenner, O. D. Sieber, M. Golling, B. W. Tilma, and U. Keller, paper presented at the CLEO, Session CW1G.6, San Jose, California, 2013.

⁹K. G. Wilcox, A. H. Quarterman, V. Apostolopoulos, H. E. Beere, I. Farrer, D. A. Ritchie, and A. C. Tropper, *Opt. Express* **20**(7), 7040–7045 (2012).

¹⁰A. H. Quarterman, K. G. Wilcox, V. Apostolopoulos, Z. Mihoubi, S. P. Elsmere, I. Farrer, D. A. Ritchie, and A. Tropper, *Nat. Photonics* **3**(12), 729 (2009).

- ¹¹P. Klopp, U. Griebner, M. Zorn, and M. Weyers, *Appl. Phys. Lett.* **98**(7), 071103 (2011).
- ¹²M. Hoffmann, O. D. Sieber, V. J. Wittwer, I. L. Krestnikov, D. A. Livshits, Y. Barbarin, T. Südmeyer, and U. Keller, *Opt. Express* **19**(9), 8108–8116 (2011).
- ¹³K. G. Wilcox, A. C. Tropper, H. E. Beere, D. A. Ritchie, B. Kunert, B. Heinen, and W. Stolz, *Opt. Express* **21**(2), 1599–1605 (2013).
- ¹⁴M. Scheller, T. L. Wang, B. Kunert, W. Stolz, S. W. Koch, and J. V. Moloney, *Electron. Lett.* **48**(10), 588–589 (2012).
- ¹⁵S. Ranta, A. Häkkinen, T. Leinonen, L. Orsila, J. Lyytikäinen, G. N. Steinmeyer, and M. Guina, *Opt. Lett.* **38**(13), 2289–2291 (2013).
- ¹⁶R. Bek, H. Kahle, T. Schwarzbäck, M. Jetter, and P. Michler, *Appl. Phys. Lett.* **103**(24), 242101 (2013).
- ¹⁷J. Rautiainen, V.-M. Korpijärvi, J. Puustinen, M. Guina, and O. G. Okhotnikov, *Opt. Express* **16**(20), 15964 (2008).
- ¹⁸A. Härkönen, J. Rautiainen, L. Orsila, M. Guina, K. Rößner, M. Hümmer, T. Lehnhardt, M. Müller, A. Forchel, M. Fischer, J. Koeth, and O. G. Okhotnikov, *IEEE Photonics Technol. Lett.* **20**(15), 1332–1334 (2008).
- ¹⁹D. J. H. C. Maas, A.-R. Bellancourt, B. Rudin, M. Golling, H. J. Unold, T. Südmeyer, and U. Keller, *Appl. Phys. B* **88**, 493–497 (2007).
- ²⁰B. Rudin, V. J. Wittwer, D. J. H. C. Maas, M. Hoffmann, O. D. Sieber, Y. Barbarin, M. Golling, T. Südmeyer, and U. Keller, *Opt. Express* **18**(26), 27582–27588 (2010).
- ²¹M. Mangold, V. J. Wittwer, C. A. Zaugg, S. M. Link, M. Golling, B. W. Tilma, and U. Keller, *Opt. Express* **21**(21), 24904–24911 (2013).
- ²²M. Mangold, C. A. Zaugg, S. M. Link, M. Golling, B. W. Tilma, and U. Keller, *Opt. Express* **22**(5), 6099–6107 (2014).
- ²³M. Mangold, S. M. Link, A. Klenner, C. A. Zaugg, M. Golling, B. W. Tilma, and U. Keller, *IEEE Photonics J.* **6**(1), 1–9 (2014).
- ²⁴J. G. McInerney, A. Mooradian, A. Lewis, A. V. Shchegrov, E. M. Strzelecka, D. Lee, J. P. Watson, M. Liebman, G. P. Carey, B. D. Cantos, W. R. Hitchens, and D. Heald, *Electron. Lett.* **39**(6), 523–525 (2003).
- ²⁵Y. Barbarin, M. Hoffmann, W. P. Pallmann, I. Dahhan, P. Kreuter, M. Miller, J. Baier, H. Moench, M. Golling, T. Südmeyer, B. Witzigmann, and U. Keller, *IEEE J. Sel. Top. Quantum Electron.* **17**(6), 1779–1786 (2011).
- ²⁶A. Harkonen, A. Bachmann, S. Arafin, K. Haring, J. Viheriala, M. Guina, and M.-C. Amann, paper presented at the SPIE Photonics Europe, Session 772015–772017, Brussels, Belgium, 2010.
- ²⁷C. Wilmsen, H. Temkin, and L. A. Coldren, *Vertical-Cavity Surface-Emitting Lasers* (Cambridge University Press, 1999).
- ²⁸E. W. Young, K. D. Choquette, S. L. Chuang, K. M. Geib, A. J. Fischer, and A. A. Allerman, *IEEE Photonics Technol. Lett.* **13**(9), 927–929 (2001).
- ²⁹W. P. Pallmann, C. A. Zaugg, M. Mangold, I. Dahhan, M. Golling, B. W. Tilma, B. Witzigmann, and U. Keller, *IEEE Photonics J.* **5**(4), 1501207 (2013).
- ³⁰K. Jasim, Q. Zhang, A. V. Nurmikko, A. Mooradian, G. Carey, W. Ha, and E. Ippen, *Electron. Lett.* **39**(4), 373–375 (2003).
- ³¹K. Jasim, Q. Zhang, A. V. Nurmikko, E. Ippen, A. Mooradian, G. Carey, and W. Ha, *Electron. Lett.* **40**(1), 34–35 (2004).
- ³²W. P. Pallmann, C. A. Zaugg, M. Mangold, V. J. Wittwer, H. Moench, S. Gronenborn, M. Miller, B. W. Tilma, T. Südmeyer, and U. Keller, *Opt. Express* **20**, 24791–24802 (2012).
- ³³H. Moench, A. Andreadaki, S. Gronenborn, J. S. Kolb, P. Loosen, M. Miller, T. Schwarz, A. M. Van Der Lee, and U. Weichmann, paper presented at the SPIE Photonics West, San Francisco, 2014.
- ³⁴D. Hillerkuss, R. Schmogrow, T. Schellinger, M. Jordan, M. Winter, G. Huber, T. Vallaitis, R. Bonk, P. Kleinow, F. Frey, M. Roeger, S. Koenig, A. Ludwig, A. Marculescu, J. Li, M. Hoh, M. Dreschmann, J. Meyer, S. B. Ezra, N. Narkiss, B. Nebendahl, F. Parmigiani, P. Petropoulos, B. Resan, A. Oehler, K. Weingarten, T. Ellermeyer, J. Lutz, M. Moeller, M. Huebner, J. Becker, C. Koos, W. Freude, and J. Leuthold, *Nat. Photonics* **5**(6), 364–371 (2011).
- ³⁵K. J. Weingarten, M. J. W. Rodwell, and D. M. Bloom, *IEEE J. Quantum Electron.* **24**, 198–220 (1988).
- ³⁶D. A. B. Miller, *IEEE J. Sel. Top. Quantum Electron.* **6**, 1312–1317 (2000).
- ³⁷G. J. Spühler, K. J. Weingarten, R. Grange, L. Krainer, M. Haiml, V. Liverini, M. Golling, S. Schon, and U. Keller, *Appl. Phys. B* **81**(1), 27–32 (2005).
- ³⁸C. A. Zaugg, Z. Sun, V. J. Wittwer, D. Popa, S. Milana, T. S. Kulmala, R. S. Sundaram, M. Mangold, O. D. Sieber, M. Golling, Y. Lee, J. H. Ahn, A. C. Ferrari, and U. Keller, *Opt. Express* **21**(25), 31548–31559 (2013).
- ³⁹M. Mangold, V. J. Wittwer, O. D. Sieber, M. Hoffmann, I. L. Krestnikov, D. A. Livshits, M. Golling, T. Südmeyer, and U. Keller, *Opt. Express* **20**(4), 4136–4148 (2012).
- ⁴⁰O. Sieber, M. Hoffmann, V. Wittwer, M. Mangold, M. Golling, B. Tilma, T. Südmeyer, and U. Keller, *Appl. Phys. B* **113**, 133 (2013).
- ⁴¹D. J. H. C. Maas, B. Rudin, A.-R. Bellancourt, D. Iwaniuk, S. V. Marchese, T. Südmeyer, and U. Keller, *Opt. Express* **16**(10), 7571–7579 (2008).